Supporting Information

Changing Charge Transfer Mode with Cobalt-Molybdenum Bimetallic Atomic Pairs for Enhanced Nitrogen Fixation

Xin Li,[a] Jin Liu,[b] Yizhen Zhang [c] and Michael K. H. Leung *[a]

[a]Ability R&D Energy Research Centre, School of Energy and Environment, City University of Hong Kong, Hong Kong, China

[b]Yellow River Institute of Eco-Environment Research, Zhengzhou, China

[c]College of Safety and Environmental Engineering, Shandong University of Science and Technology, Qingdao, China

*Corresponding author:

E-mail addresses: mkh.leung@cityu.edu.hk (M. Leung)

Fig. S1. (a-b) The color of the samples obtained from Co-Mo-Zn-SA/ZIF to Co-Mo-SA/NC; (c-d) The color of the samples obtained from Co-Zn-SA/ZIF to Co-SA/NC; (e-f) The color of the samples obtained from Mo-Zn-SA/ZIF to Mo-SA/NC; (g-h) The color of the samples obtained from Co-Mo-Zn-NP/ZIF to Co-Mo-NP/NC.

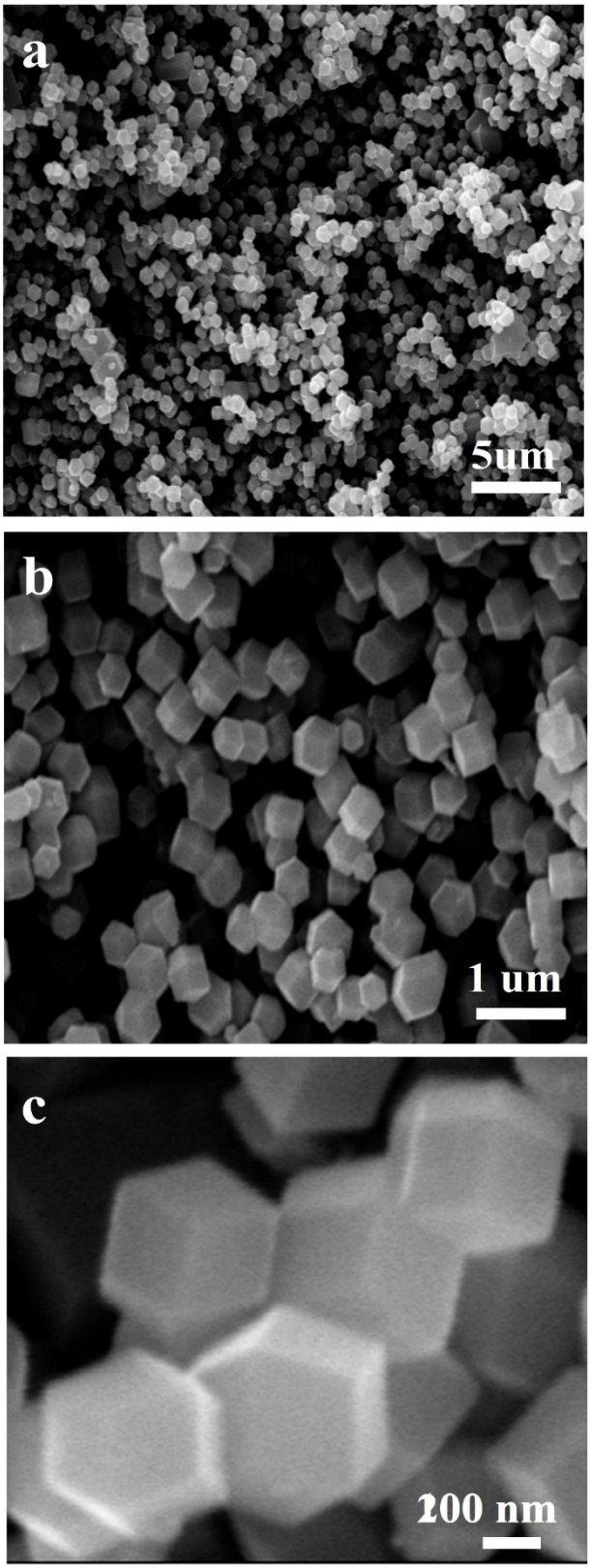

Fig. S2. (a-c) SEM images of Co-Mo-SA/NC.

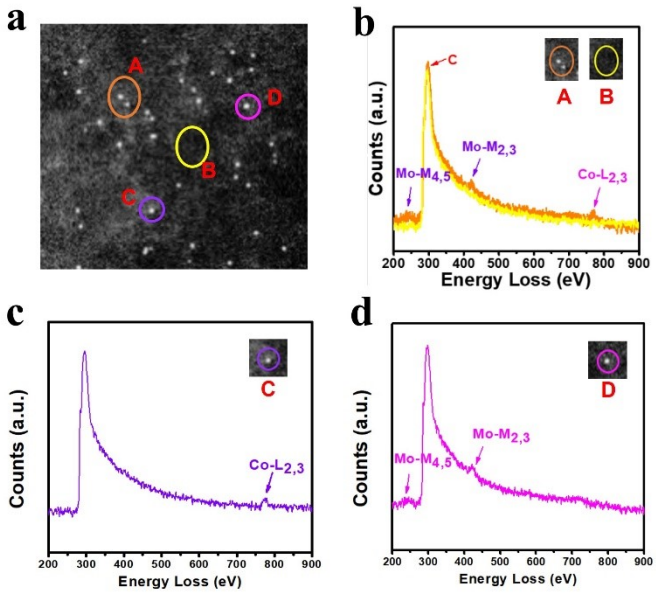

Fig. S3. (a) Atomic resolution HAADF-STEM image of Co-Mo-SA/NC; (b) the Mo-$M_{4,5}$ edge, Mo-$M_{2,3}$ edge, and Co-$L_{2,3}$ edge can be simultaneously detected on an Co-Mo atomic pair; (c) The Co-$L_{2,3}$ edge can be detected on a Co single atom; (d) The Mo-$M_{4,5}$ edge and Mo-$M_{2,3}$ edge can be detected on a Mo single atom.

To identify the composition of individual single atoms and bimetallic atomic pairs shown in the STEM images. the atomic-resolution high-angle annular dark-field transmission electron microscope (HAADF-STEM) has been performed. As shown in the Fig. S3, the Mo-$M_{4,5}$ edge, Mo-$M_{2,3}$ edge, and Co-$L_{2,3}$ edge can be simultaneously detected on an atomic pair highlighted by circle A, which can clearly prove the existence of Co-Mo atomic pairs in the Co-Mo-SA/NC. In contrast, only Mo-M edge or Co-L edge can be detected on individual single atoms highlighted by highlighted by circle C or D, which can confirm some individual Co or Mo single atom are distributed on the N-doped carbon substrate.

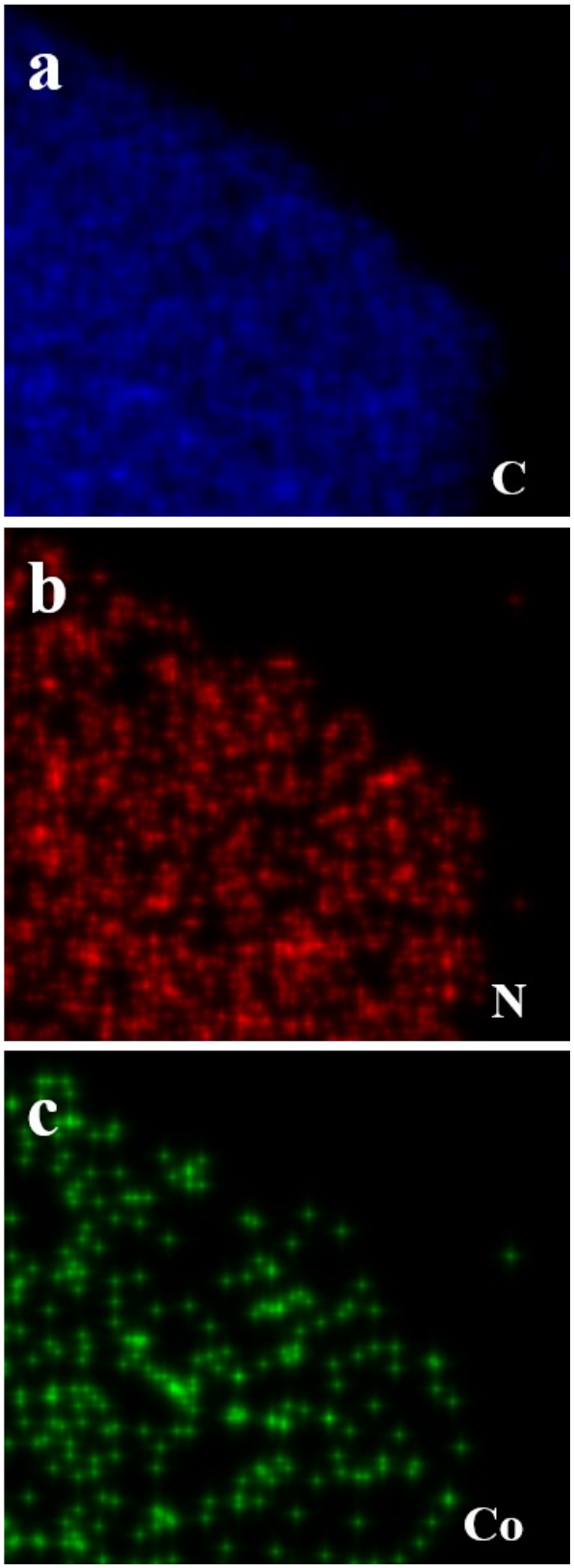

Fig. S4. EDS mappings of the corresponding C, N, Co elements for Co-SA/NC.

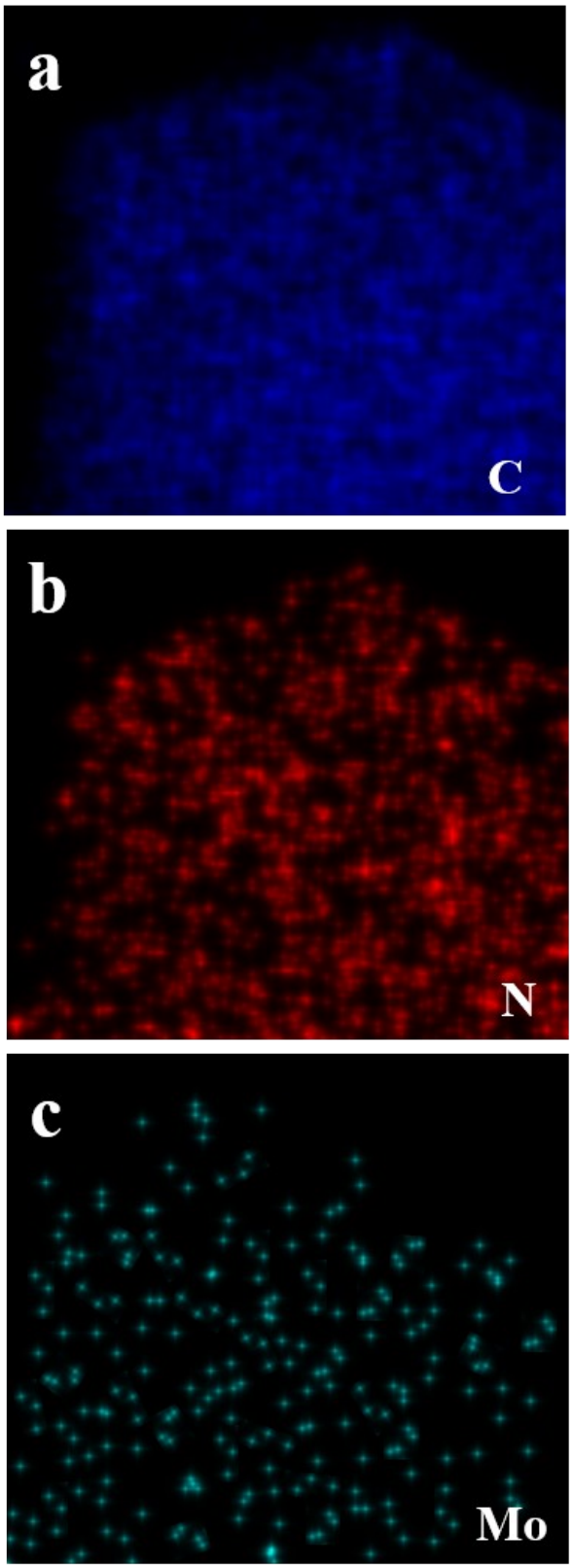

Fig. S5. EDS mappings of the corresponding C, N, Mo elements for Mo-SA/NC.

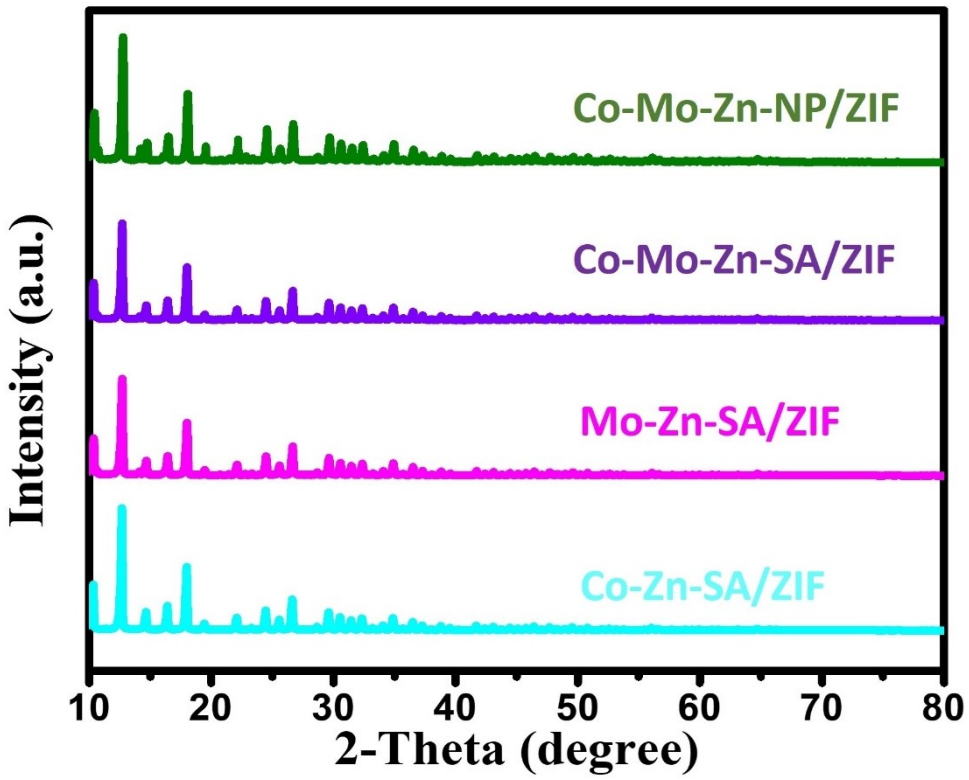

Fig. S6. XRD patterns of the Co-Mo-Zn-NP/ZIF, Co-Mo-Zn-SA/ZIF, Mo-Zn-SA/ZIF and Co-Zn-SA/ZIF.

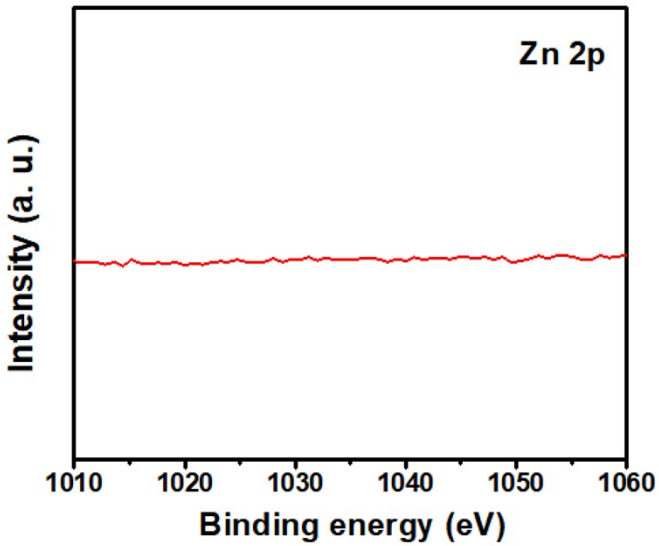

Fig. S7. High-resolution spectra of the Zn 2p XPS peak of Co-Mo-SA/NC.

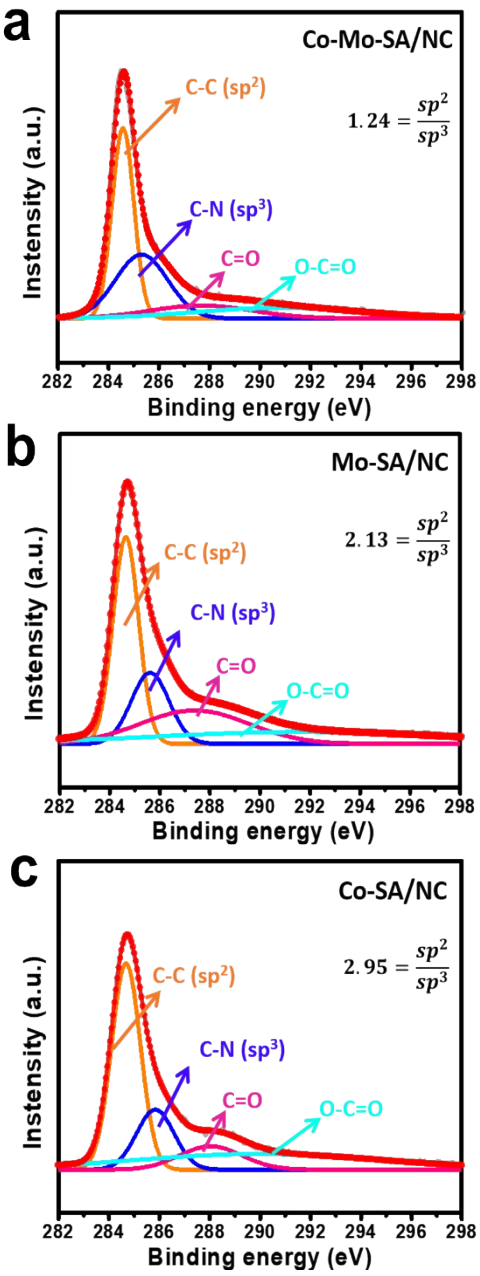

Fig. S8. High-resolution spectra of the C1s XPS peak of Co-Mo-SA/NC, Mo-SA/NC and Co-SA/NC.

It is known that carbon materials contain two types of carbon atoms (the basal-plane sp^2 carbon atoms and the defect sp^3 carbon atoms) and the degree of the defect can be measured by the sp^3 content. Compared with Co-SA/NC and Mo-SA/NC, the sp^2/sp^3 values of Co-Mo-SA/NC decreased from 2.95 and 2.13 to 1.24, respectively, indicating that there are more defects in Co-Mo-SA/NC catalysts.

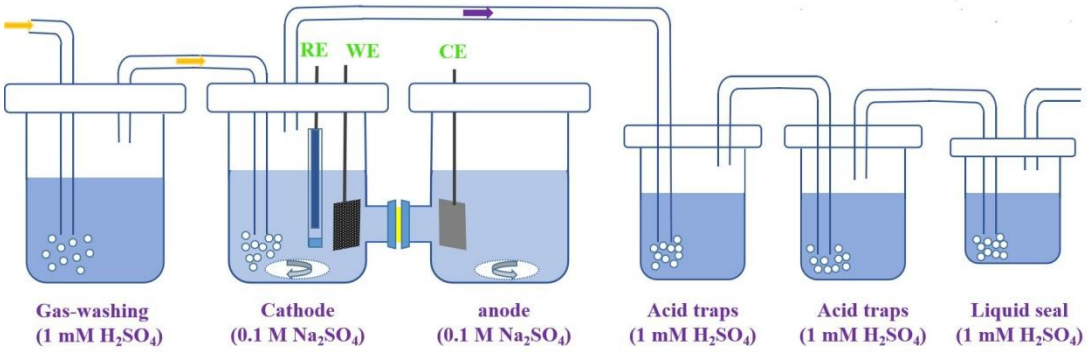

Fig. S9. Schematic diagram of the electrochemical setup.

In this work, the electrocatalytic activity of all the samples were measured in a typical gas-tight H-type cell under ambient conditions, which is the most widely investigated type in electrochemical nitrogen reduction reaction. Fig. S9 shows all the components in our NRR system, where the working and the reference electrodes were located in the cathode chamber and counter electrode was located in the anode. The two chambers of the H-type cell were separated by a Nafion membrane, and both were filled with 0.1 M Na_2SO_4 solution. Before entering the electrolytic cell, the gases were passed through 1 mM H_2SO_4 to remove any possible ammonia or nitrogen oxide pollutants. Then, the gases entered the cathode chamber for nitrogen reduction reaction. Finally, two additional reactors filled with 1 mM H_2SO_4 were connected to the end of the H-cell to capture any undissolved ammonia. It is important to note that all electrochemical cell setups (cells, membrane, flow lines, electrodes, caps) should be thoroughly cleaned with 1 M H_2SO_4 before use, and then socked in deionized water when not in use.

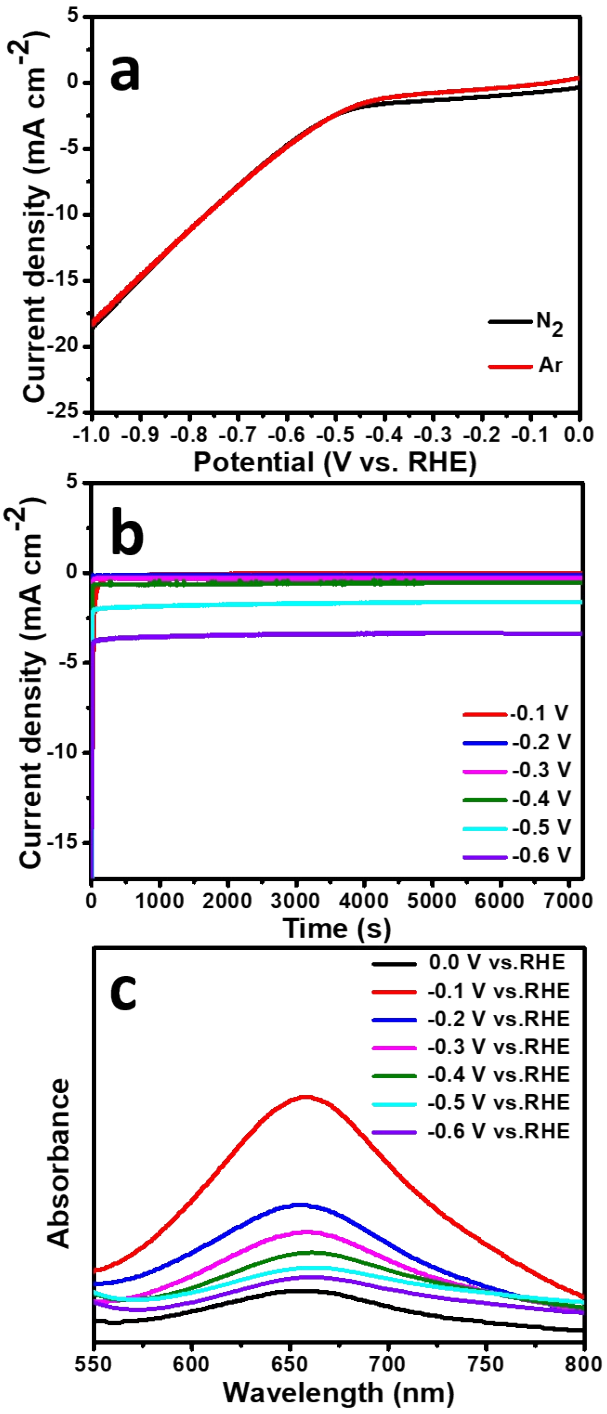

Fig. S10. (a) Linear sweep voltammetric curves of the Co-Mo-SA/NC in N_2-saturated and Ar-saturated electrolytes; (b) Chronoamperometric curves of the Co-Mo-SA/NC catalysts measured at a series of applied potentials; (c) Ultraviolet-visible absorption spectra of the Co-Mo-SA/NC at different applied potentials.

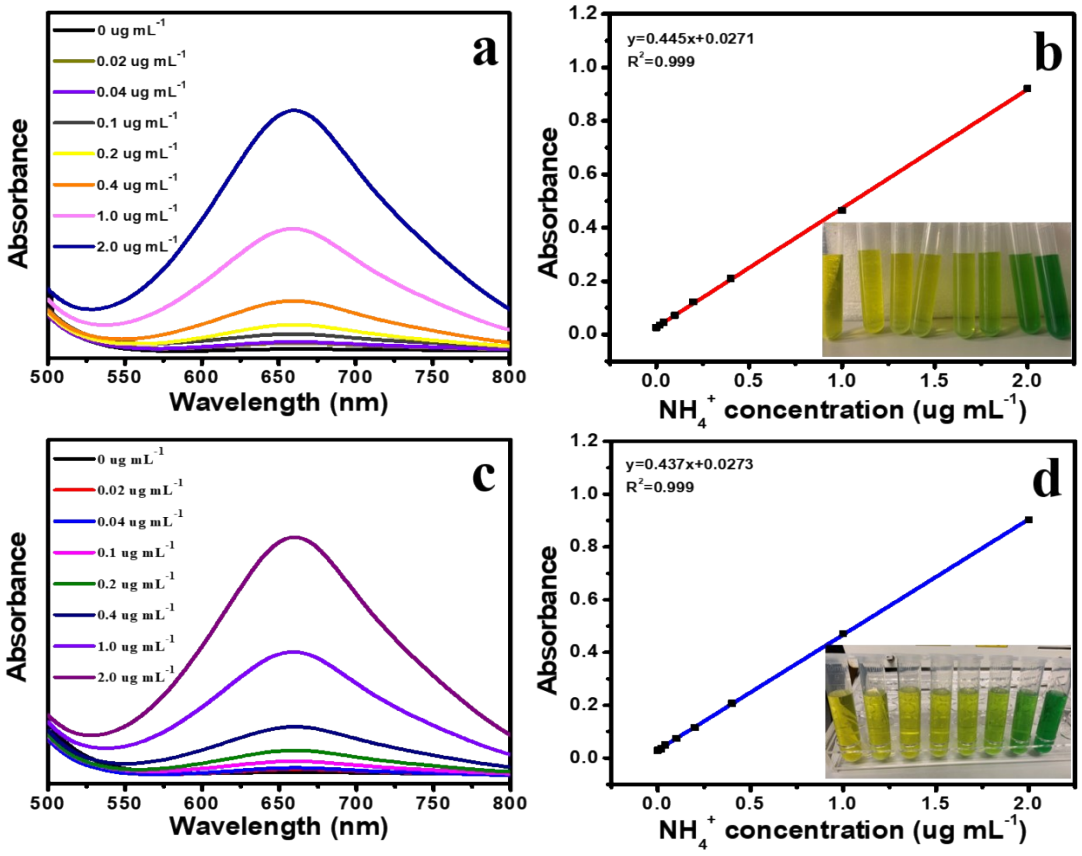

Fig. S11. Ammonia quantification using the indophenol blue method. The UV-vis absorption spectra and corresponding calibration curves for the colorimetric NH_3 in different background solutions: (a-b) 0.1 M Na_2SO_4; (c-d) 0.1 mM H_2SO_4.

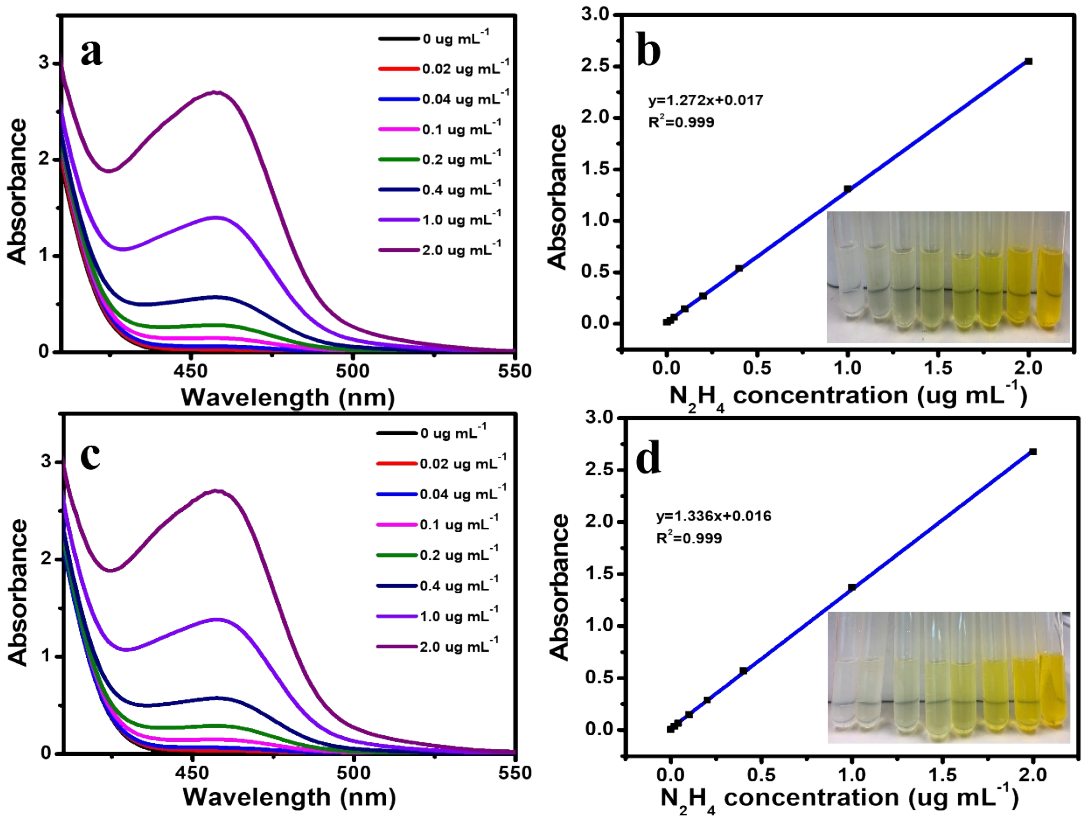

Fig. S12. (a) The UV-vis absorption spectra and (b) corresponding calibration curves for the colorimetric N_2H_4 assay in 0.1 M Na_2SO_4; (c)The UV-Vis absorption spectra and (d) corresponding calibration curves for the colorimetric N_2H_4 assay in 0.1 mM H_2SO_4.

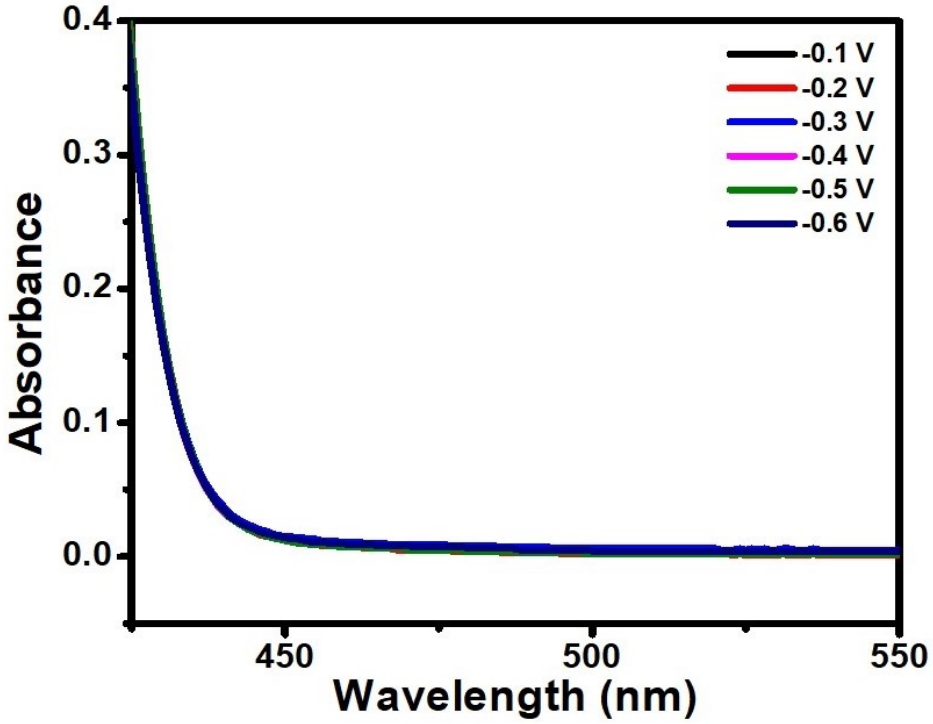

Fig. S13. UV-vis absorption spectra of the detected electrolyte with Co-Mo-SA/NC catalyst stained with the indicator for $N_2H_4 \cdot H_2O$.

It can be seen that no signals of N_2H_4 can be detected.

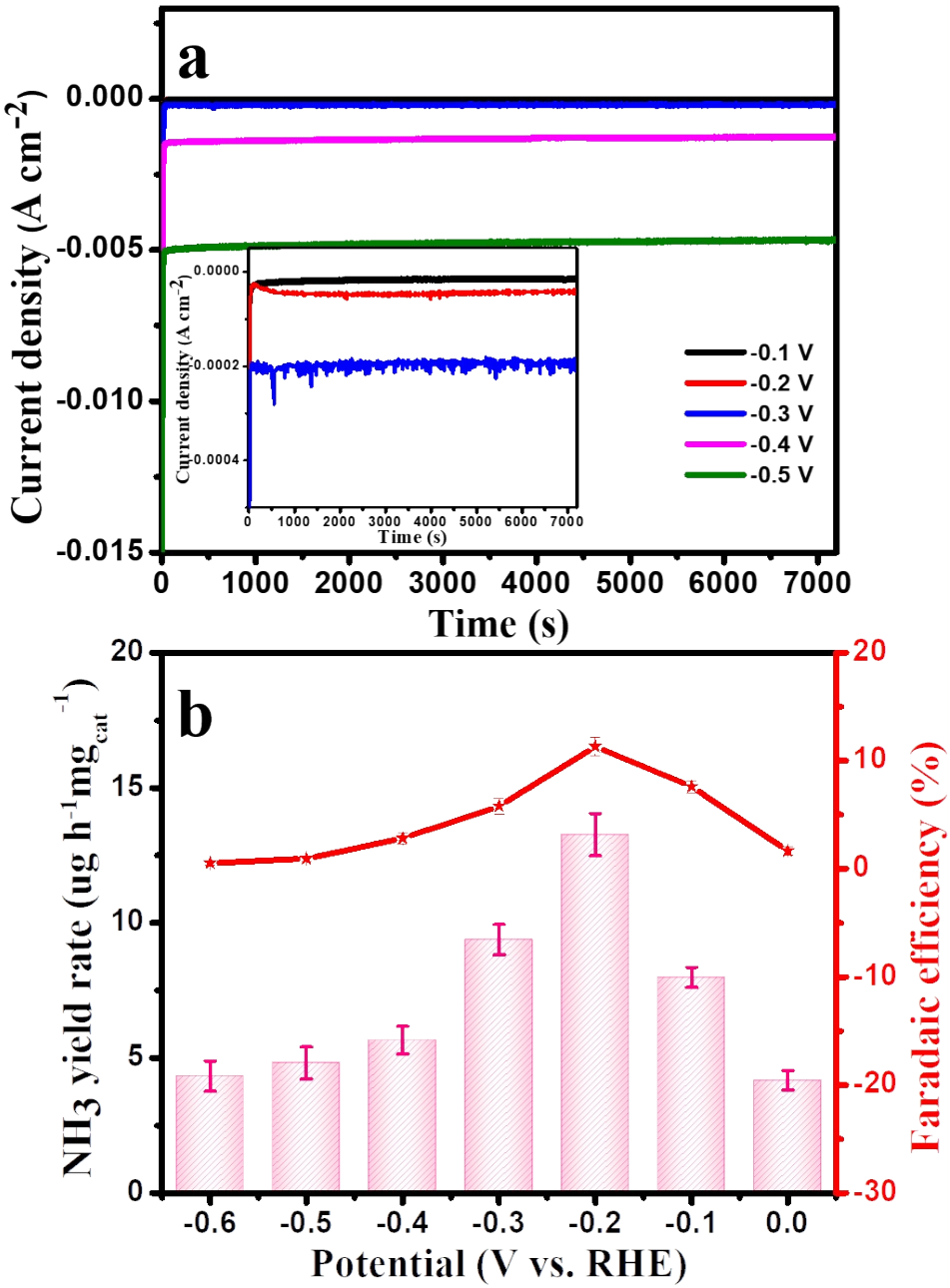

Fig. S14. NRR electrochemical performances of Co-SA/NC under ambient conditions. (a) Chronoamperometric curves of Co-SA/NC at different potentials in 0.1 M Na_2SO_4; (b) NH_3 yield rates and FEs of Co-SA/NC at different potentials.

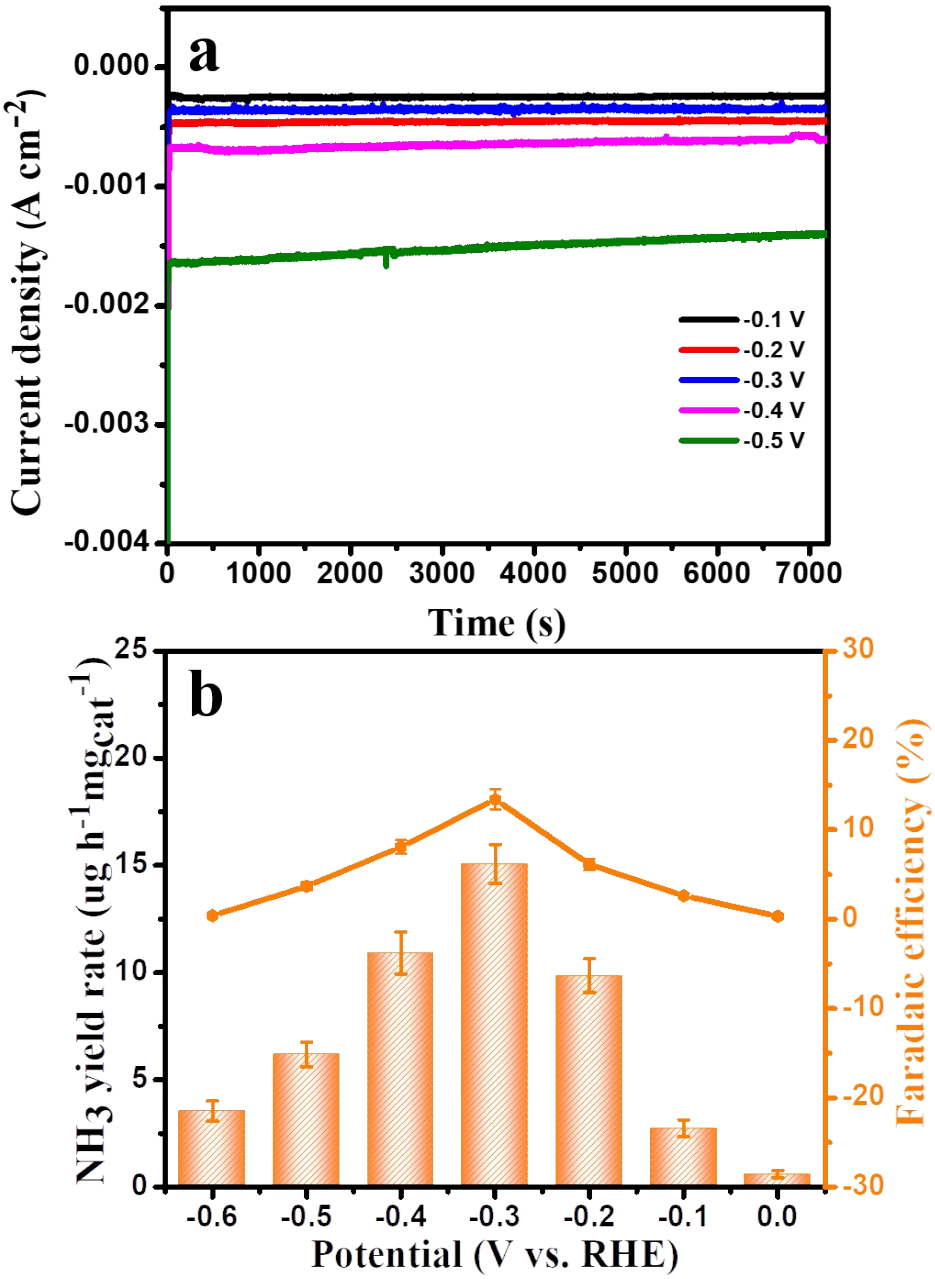

Fig. S15. NRR electrochemical performances of Mo-SA/NC under ambient conditions. (a) Chronoamperometric curves of Mo-SA/NC at different potentials in 0.1 M Na_2SO_4; (b) NH_3 yield rates and FEs of Mo-SA/NC at different potentials.

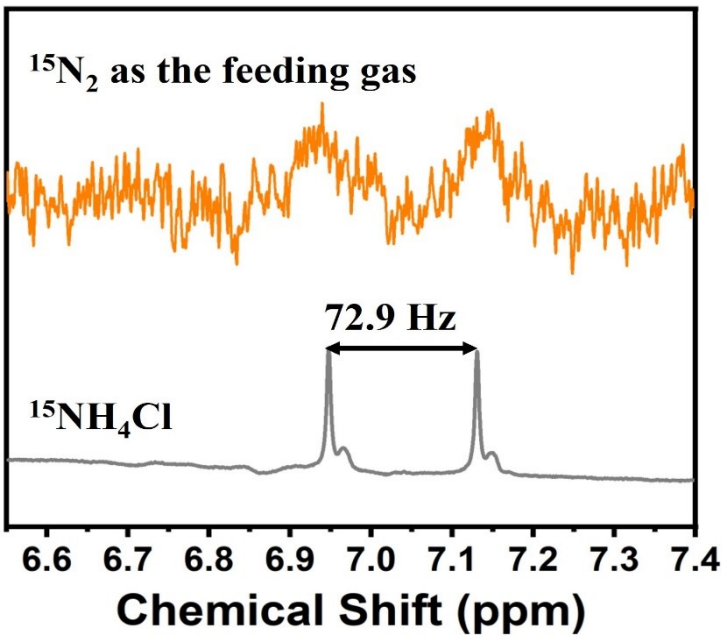

Fig. S16. ^{1}H NMR spectra (400 MHz) of $^{15}NH_4^+$ produced from the NRR reaction (at -0.1 V vs. RHE) using $^{15}N_2$ as the N_2 source.

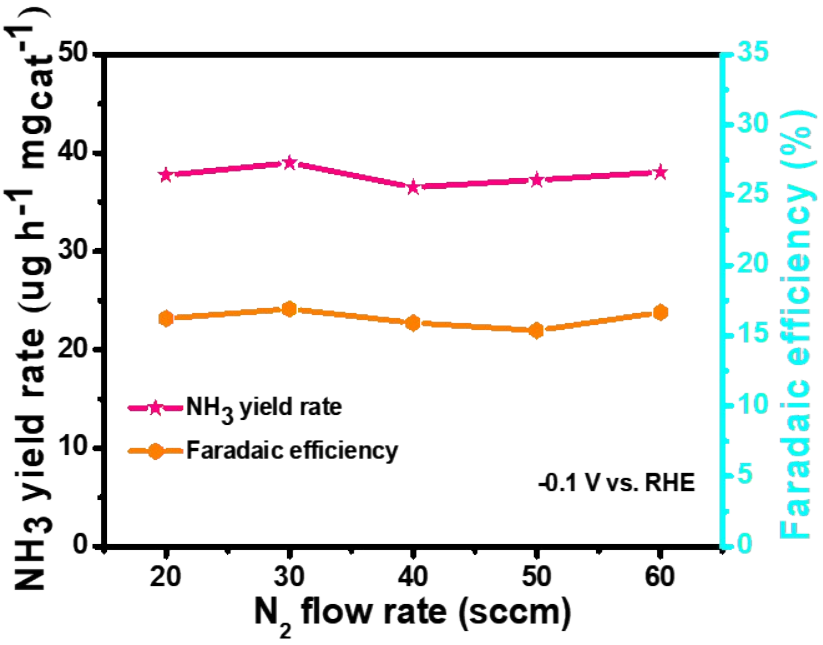

Fig. S17. NH_3 yield rates and Faradaic efficiencies of Co-Mo-SA/NC at different N_2 flow rates.

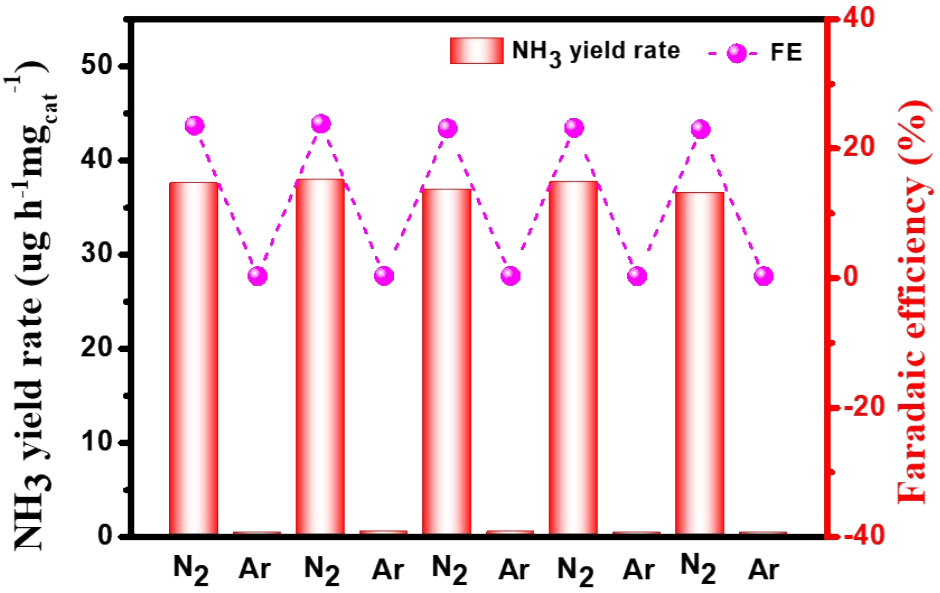

Fig. S18. NH_3 yield rates and Faradaic efficiencies of Co-Mo-SA/NC at -0.1 V (vs. RHE) with alternating cycles at the interval of 2 h between N_2-saturated and Ar-saturated electrolytes.

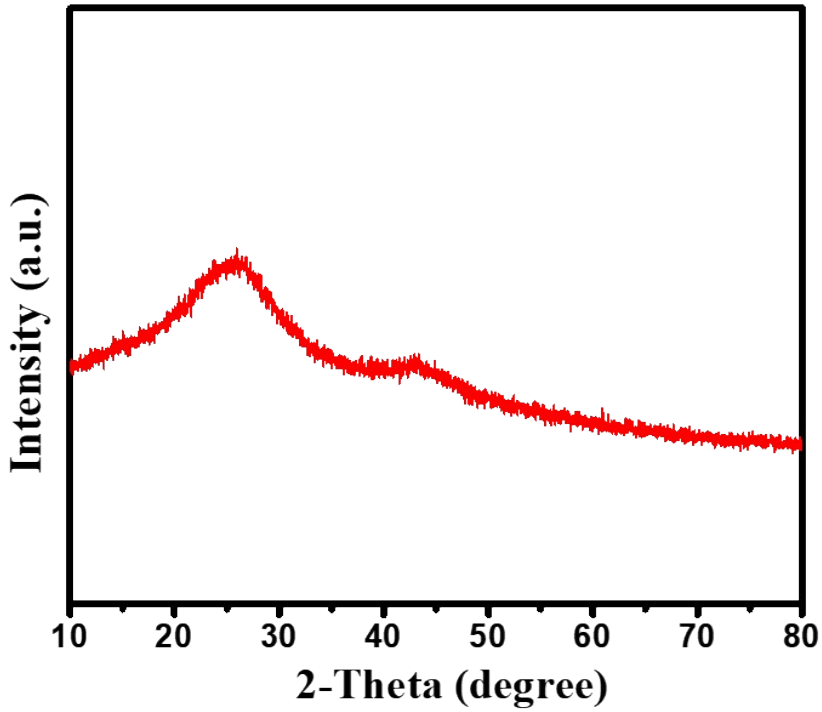

Fig. S19. XRD image of Co-Mo-SA/NC after the 24 h electrolytic NRR.

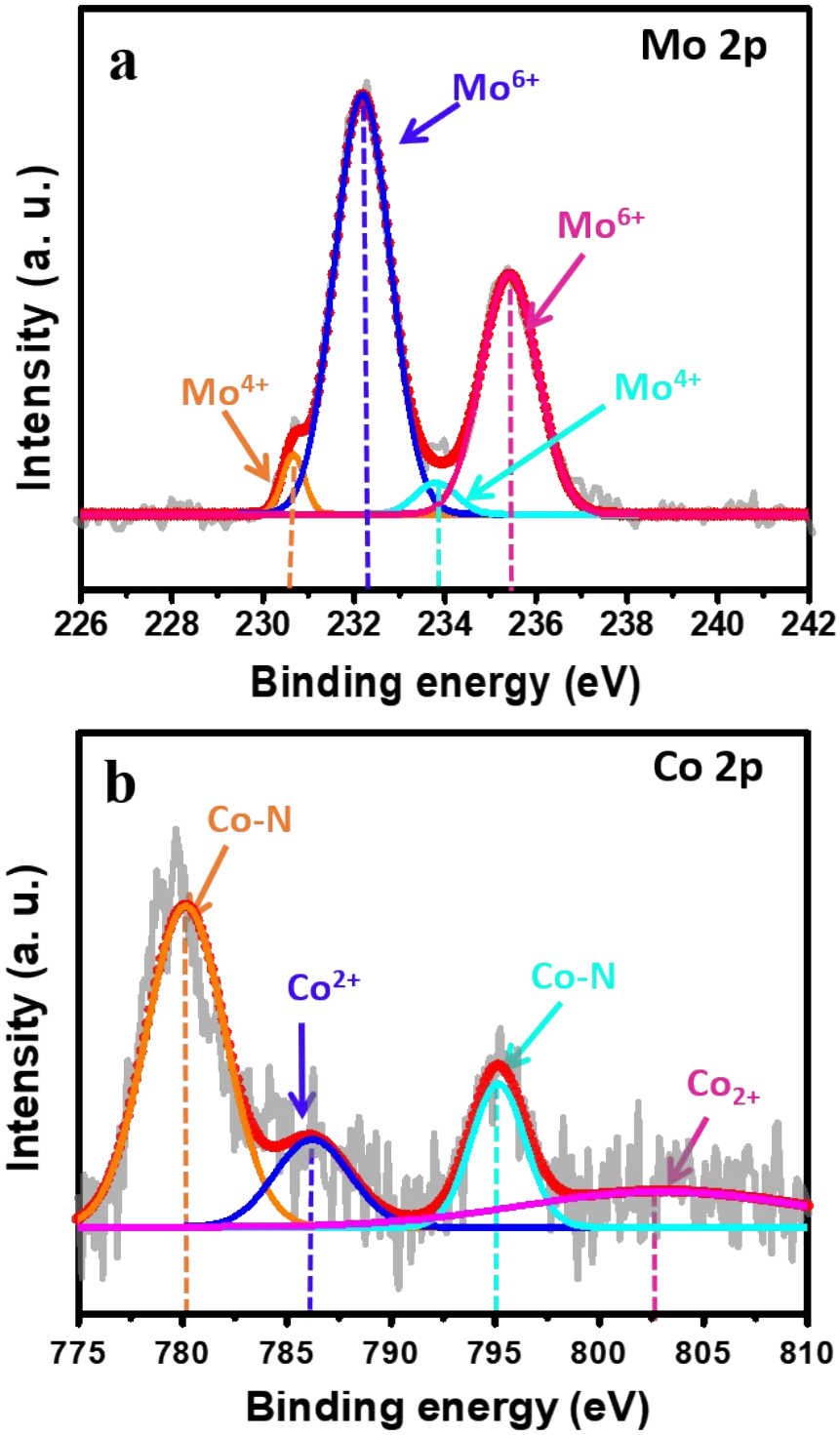

Fig. S20. XPS spectrums of Co-Mo-SA/NC after the 24 h electrolytic NRR.

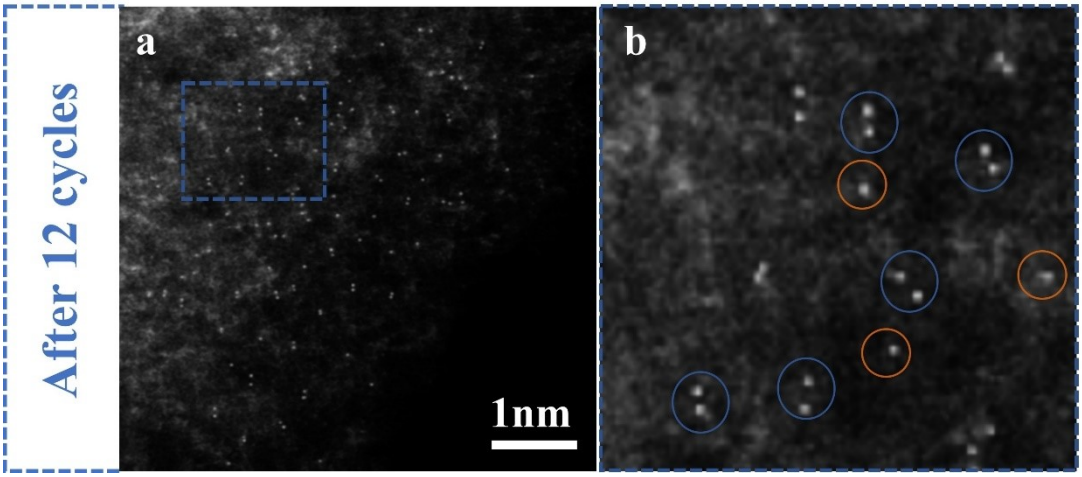

Fig. S21. (a-b) HAADF-STEM images of Co-Mo-SA/NC after the 24 h electrolytic NRR.

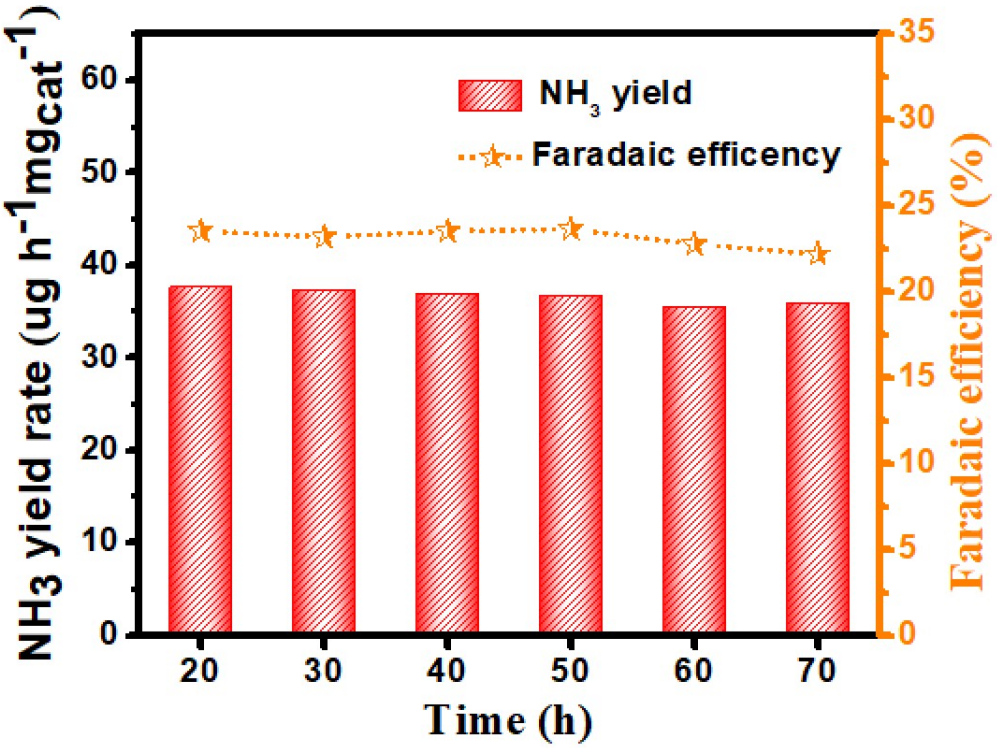

Fig. S22. The durability measurement of Co-Mo-SA/NC catalyst at -0.1 versus RHE for 70 h.

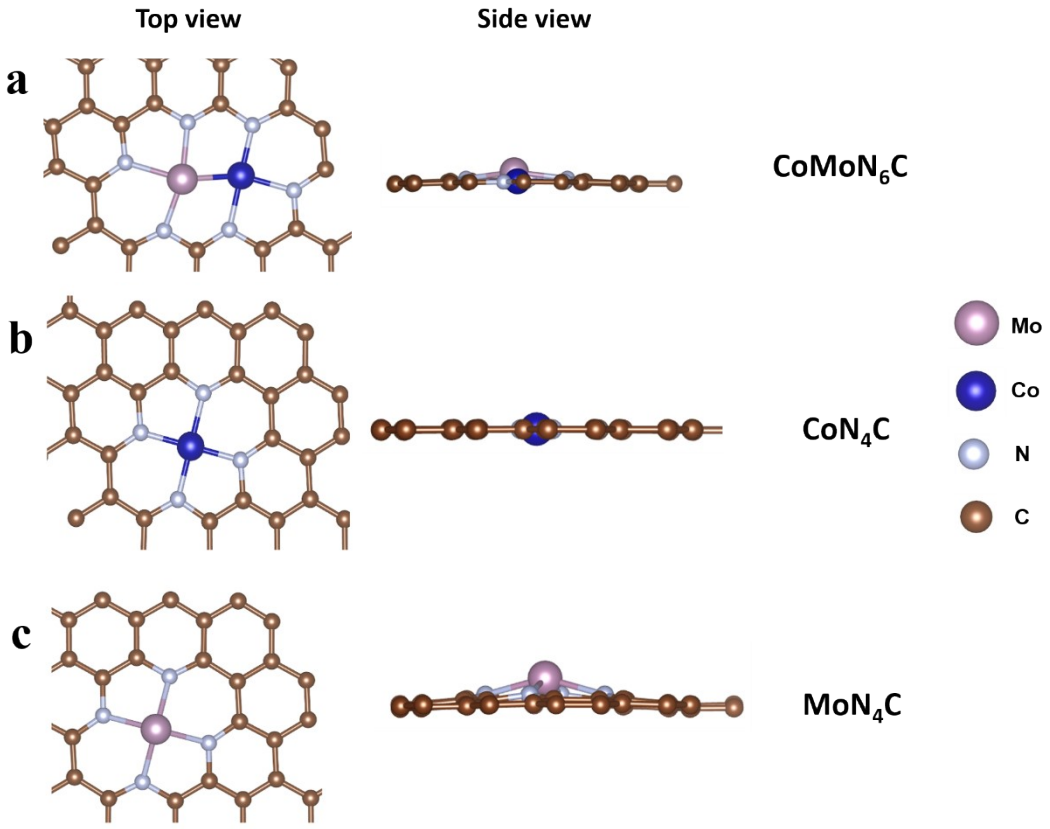

Fig. S23. (a) The optimized structure of Co-Mo-SA/NC; (b) The optimized structure of Co-SA/NC; (c) The optimized structure of Mo-SA/NC.

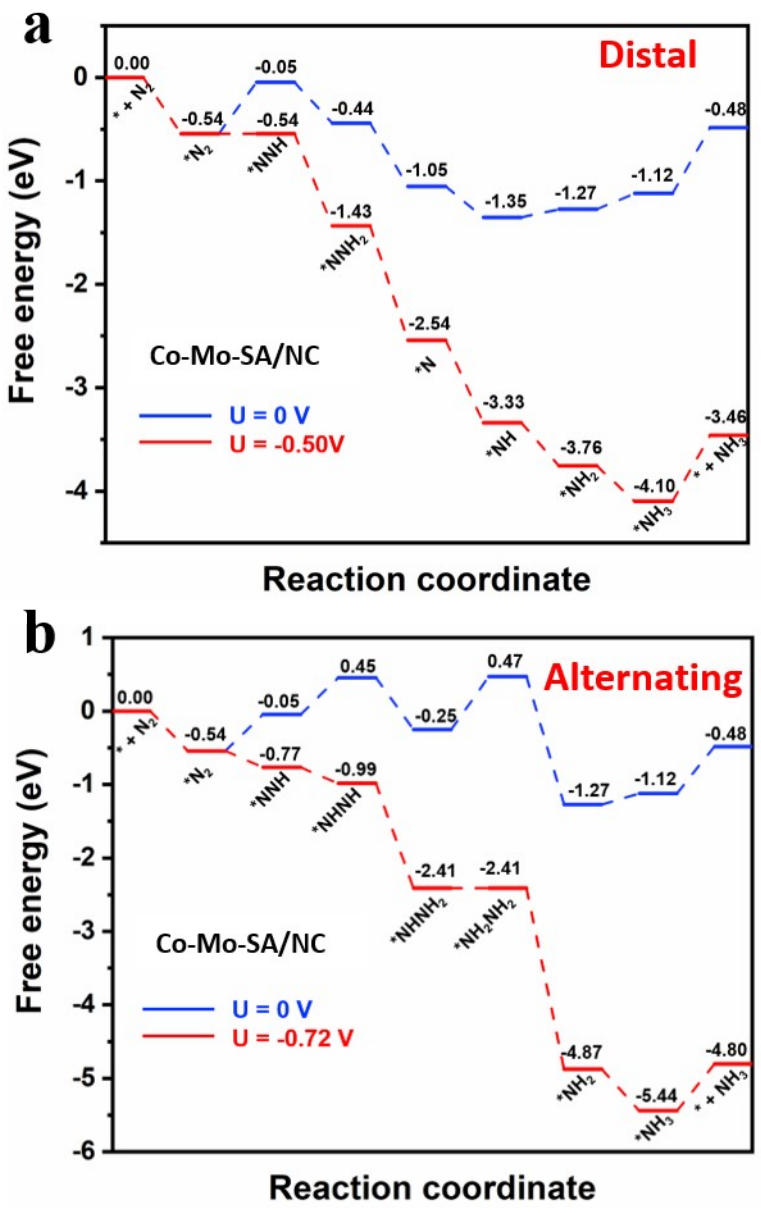

Fig. S24. Free-energy diagrams for NRR on $CoMoN_6C$ structure at zero and applied potential (limiting potential) through (a) distal; and (b) alternating pathways.

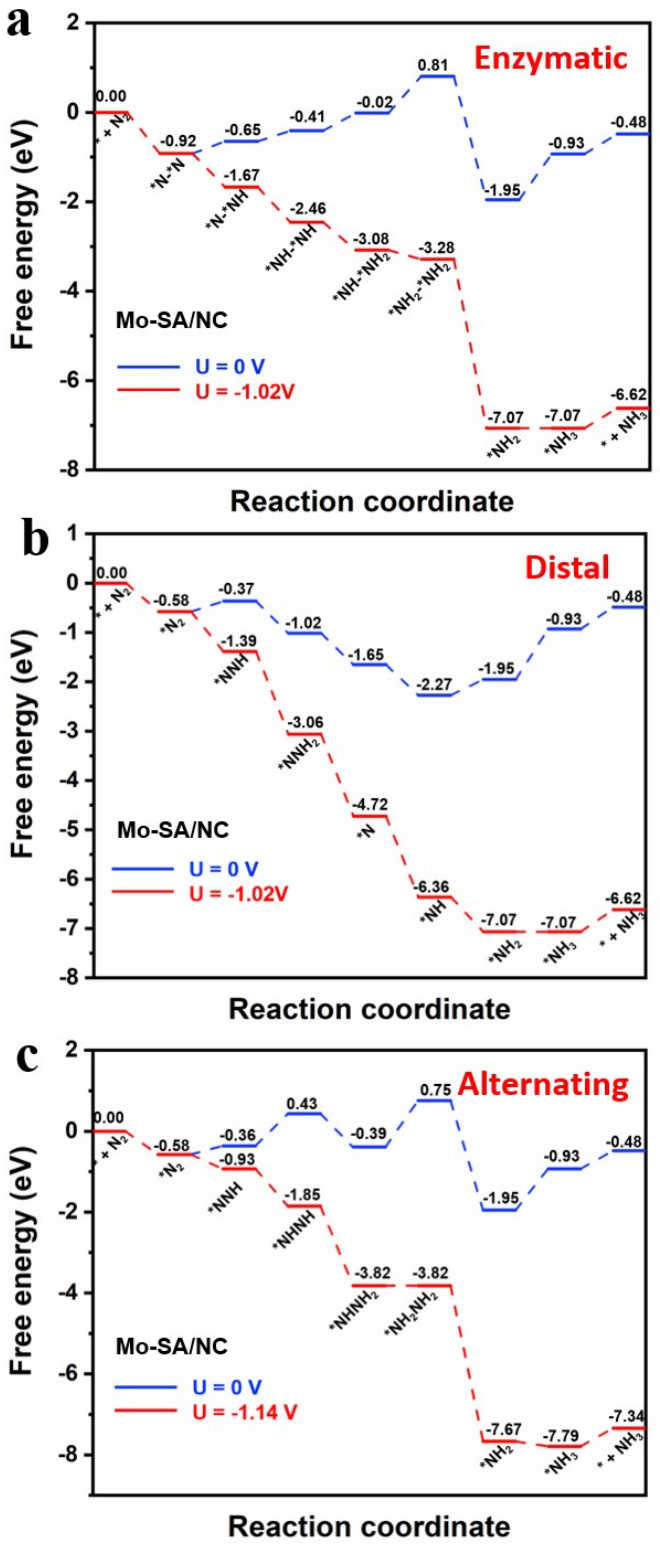

Fig. S25. Free-energy diagrams for NRR on MoN_4C structure at zero and applied potential (limiting potential) through (a) enzymatic; (b)distal; and (c) alternating pathways.

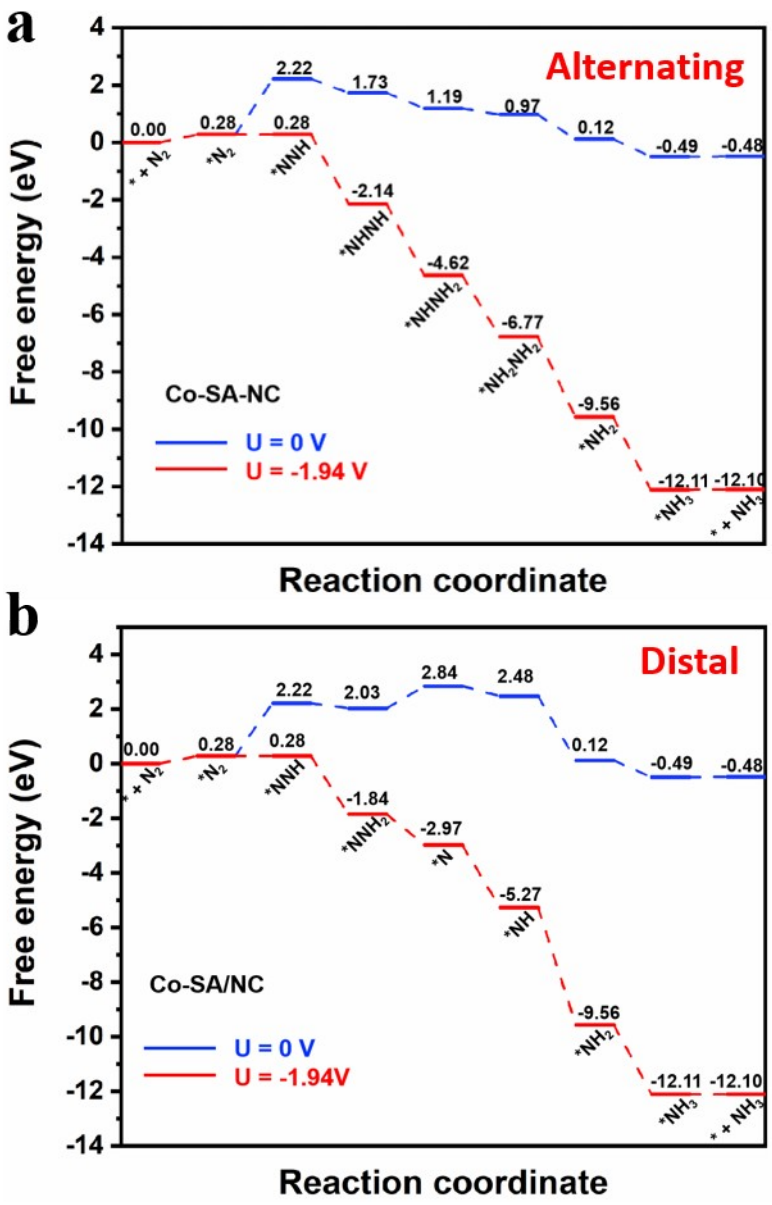

Fig. S26. Free-energy diagrams for NRR on CoN_4C structure at zero and applied potential (limiting potential) through a) alternating and b) distal pathways.

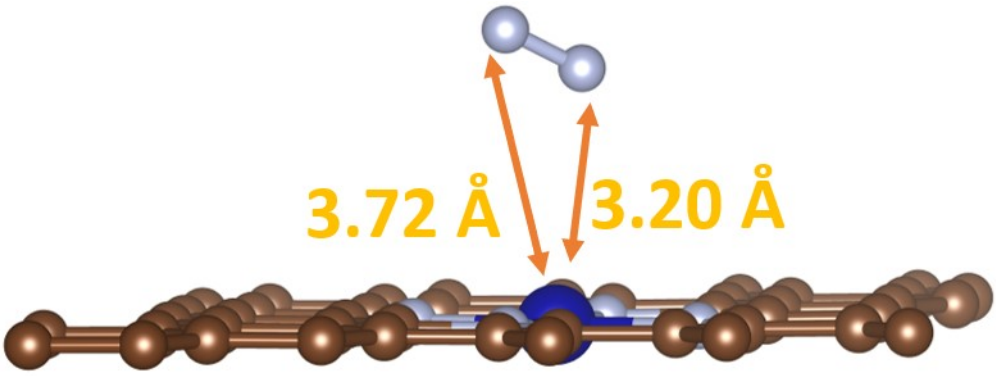

Fig. S27. The optimized distance between N_2 and Co on Co-SA/NC for enzymatic pathway.

Note: When calculating the NRR enzymatic mechanism on CoN_4C, we found that the N_2 will not be absorbed on the Co atom in a "side on" format. As shown in the figure above, the optimized distance between N_2 and Co atom are 3.20 Å and 3.72 Å, which are larger than the common Co-N bond distance of about 2.1 Å, indicating N_2 will be preferentially absorbed on CoN_4C with the "end on" format. Therefore, we only discuss the "end on" mechanism of NRR on the CoN_4C model in this work.

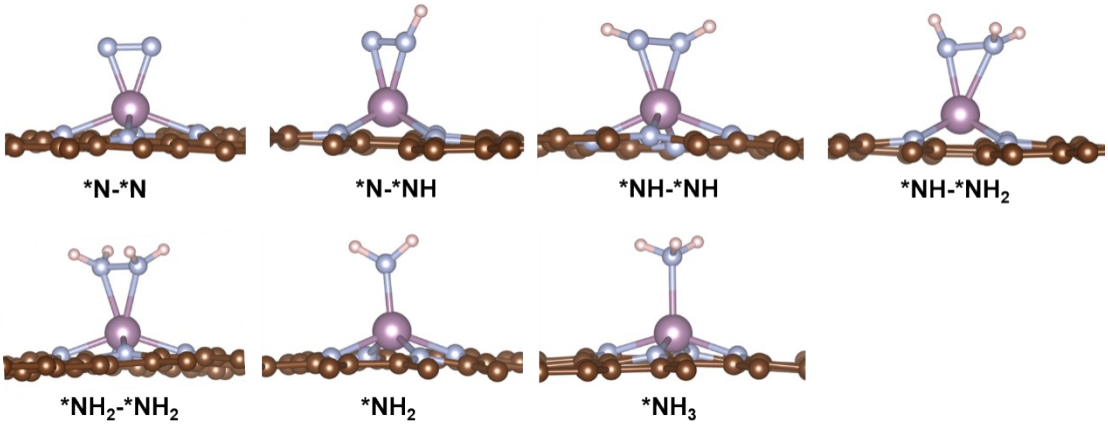

Fig. S28. Optimized intermediates configurations on Mo-SA/NC for enzymatic pathway.

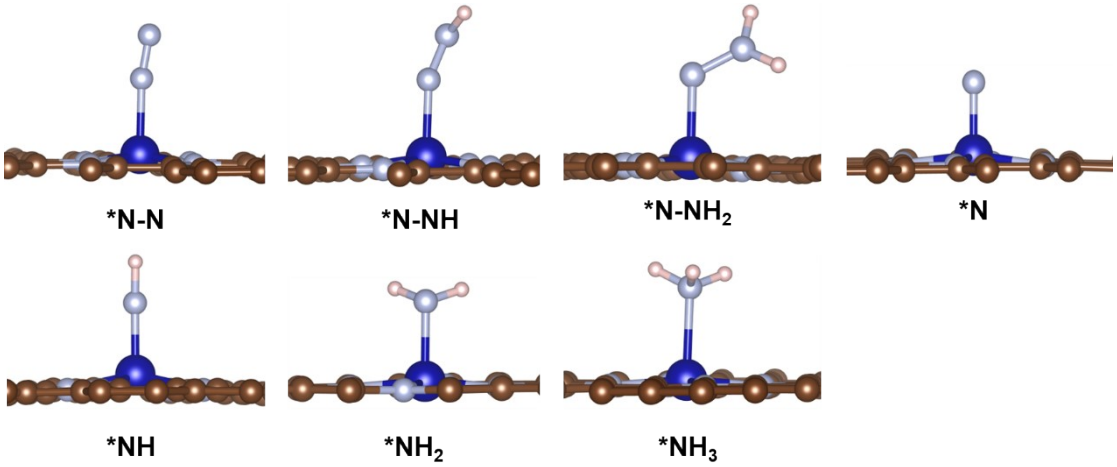

Fig. S29. Optimized intermediates configurations on Co-SA/NC for enzymatic pathway.

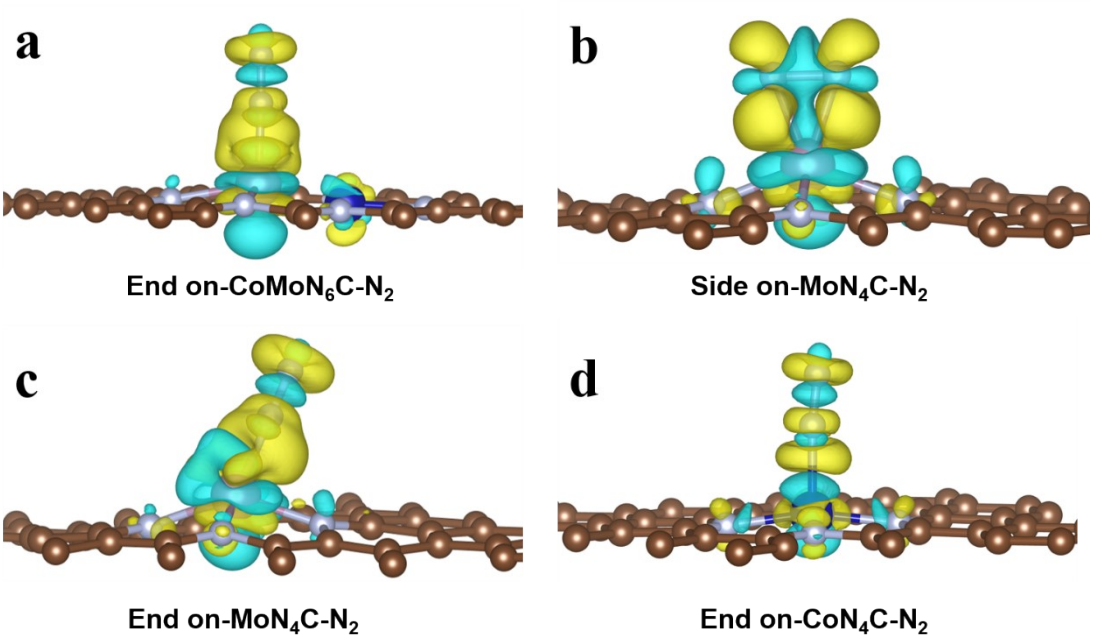

Fig. S30. Charge density difference of the adsorption of N_2 via side-on configuration on different structures.

Table S1. The metal contents of Co-Mo-SA/NC, Co-SA/NC, Mo-SA/NC, Co-Mo-NP/NC and N/C.

Catalyst	Mo metal loading (wt%)	Co metal loading (wt%)
Co-Mo-SA/NC	0.45	0.71
Co-SA/NC	0	1.03
Mo-SA/NC	0.87	0
Co-Mo-NP/NC	1.25	1.49
N/C	0	0

Table S2. Comparisons of NRR performances for Co-Mo-SA/NC with recently reported electrocatalysts working in the aqueous electrolyte.

Catalyst	Electrolyte	Potential V (vs. RHE)	NH_3 yield rate ($\mu g\ h^{-1}\ mg^{-1}$)	Faradaic Efficiency	Reference
Metal-free Electrocatalysts					
B_4C nanosheet	0.1 M HCl	-0.75	26.57	15.95%	1
BP	0.1 M HCl	-0.6	26.24	12.7%	2
BP NSs	0.1 M KOH	-0.6	31.37	5.07%	3
BNS/CP	0.1 M Na_2SO_4	-0.8	13.22	4.04%	4
B-doped graphene	0.05 M H_2SO_4	-0.5	9.8 $\mu g\ h^{-1}\ cm^{-2}$	10.8%	5
N-doped carbon	0.05 M H_2SO_4	-0.9	23.8	1.42%	6
F-doped carbon	0.05 M H_2SO_4	-0.55	6.9 $\mu g\ h^{-1}\ cm^{-2}$	12.1%	7
Polymeric CN	0.1 M HCl	-0.2	8.09	11.59%	8
BCN	0.05 M Na_2SO_4	-0.6	8.39 $\mu g\ h^{-1}\ cm^{-2}$	3.87%	9
$S_{6.23}$-$B_{8.09}$/CNFs	0.5 M K_2SO_4	-0.7	0.223 $\mu mol\ h^{-1}\ cm^{-2}$	22.4%	10
Precious Metal Electrocatalysts					
Pd cubes	0.1 M Li_2SO_4	0	24.3	36.6%	11
np-$PdH_{0.43}$	0.1 M PBS	-0.15	20.4	43.6%	12
Au_6/Ni	0.05 M H_2SO_4	-0.14	7.4	67.8%	13
pAu/Ni foam	0.1 M Na_2SO_4	-0.2	9.42 $\mu g\ h^{-1}\ cm^{-2}$	13.36%	14
Au/TiO_2	0.1 M HCl	-0.2	21.4	8.11%	15
Au/CoO_X	0.05 M H_2SO_4	-0.5	15.1 $\mu g\ h^{-1}\ cm^{-2}$	19%	16
hollow Au nanocages	0.5 M $LiClO_4$	-0.4	3.9 $\mu g\ h^{-1}\ cm^{-2}$	30.2%	17
Pd/C	0.1 M PBS	-0.1	4.5 $ug\ h^{-1}\ mg_{Pd}^{-1}$	8.2%	18
etched-PdZn/ NHCP	0.1 M PBS	-0.2	5.28	16.9%	19
CuAu@Cu	0.1 M HCl	-0.2	33.9	24.1%	20
$Pd_{0.2}Cu_{0.8}$/rGO	0.1 M KOH	-0.2	2.8	4.5%	21

Pd_3Bi	0.05 M H_2SO_4	-0.2	59.05	21.52%	[22]
Pd_3Cu_1 alloys	1 M KOH	-0.25	39.9	1.22%	[23]
THH Au NRs	0.1 M KOH	-0.2	1.648 μg h^{-1} cm^{-2}	4.02%	[24]
α-Au/CeO_X-rGO	0.1 M HCl	-0.2	8.3	10.1%	[25]
RuFeCoNiCu/CP	0.1 M KOH	-0.05	11.4 μg h^{-1} cm^{-2}	38.5%	[26]
Ru@ZrO_2/ NC	0.1 M HCl	-0.21	3.665 mg h^{-1} mg_{Ru}^{-2}	21%	[27]
Ru/MoS_2	0.01 M HCl	-0.15	1.14×10^{-10}mol $cm^{-2}s^{-1}$	17.6%	[28]
Ag nanosheets	0.1 M HCl	-0.6	2.8 μg h^{-1} cm^{-2}	4.8%	[29]
Rh nanosheet	0.1 M KOH	-0.2	23.88	0.217%	[30]
Transition Metal Electrocatalysts					
W-NO/NC	0.5 M $LiClO_4$	-0.7	12.62	8.35%	[31]
W_2N_3	0.1 M HCl	-0.2	11.66±0.98	11.67±0.93%	[32]
$Bi_4V_2O_{11}/CeO_2$	0.1 M HCl	-0.2	23.21	10.16%	[33]
$BiVO_4$	0.2 M Na_2SO_4	-0.5	8.6	10.04%	[34]
FeNi@C	0.1 M Na_2SO_4	-0.5	1.72×10^{-10}mol s^{-1} cm^{-2}	23%	[35]
Mo_3Fe_3C	0.1 M Li_2SO_4	-0.05	72.5 umol h^{-1} g^{-1}	27%	[36]
Mo-FeP	0.1 M HCl	-0.3	13.1	7.49%	[37]
Fe_2O_3-CNT	$KHCO_3$	-1.0	0.22	0.15%	[38]
FePc/C	0.1 M Na_2SO_4	-0.3	10.25	10.5%	[39]
Co-doped carbon	0.001 M H_2SO_4	-0.2	0.97	4.2%	[40]
FeMoS	0.1 M HCl	-0.5	8.45	2.96	[41]
Mo_2C/C	0.05 M Li_2SO_4	-0.3	11.3 ug h^{-1} mg_{Mo2C}^{-1}	7.8%	[42]
MoS_2 nanoflower	0.1 M Na_2SO_4	-0.4	29.28	8.34%	[43]
MoS_2/C_3N_4	0.1 M Na_2SO_4	-0.5	19.86	6.87%	[44]

MoS_2 nanosheet	0.1 M Li_2SO_4	-0.2	43.4	9.81%	[45]
Mo nanofilm	0.01 M H_2SO_4	-0.14	1.89	0.72%	[46]
C-Ti_xO_y/C	0.1 M $LiClO_4$	-0.4	14.8	17.8%	[47]
Zr-TiO_2	0.1 M KOH	-0.45	8.9	17.3%	[48]
TiO_2/$Ti_3C_2T_x$	0.1 M HCl	-0.55	32.17	16.07%	[49]
NiTe/C	0.1 M HCl	-0.1	33.34	17.38%	[50]
Cu/PI	0.1 M KOH	-0.3	12.4	6.56%	[51]
CoS_2/NS-G	0.05 M H_2SO_4	-0.3	25	25.9%	[52]
Co/NC	0.05 M H_2SO_4	-0.9	37.6	17.6%	[53]
PC/Sb/$SbPO_4$	0.1 M HCl	-0.15	25	31%	[54]
TiO_2 NAs	0.1 M Na_2SO_4	-0.55	4.19×10^{-10}mol s^{-1} cm^{-2}	20.3%	[55]
Fe-doped MoO_3	0.1 M Na_2SO_4	-0.7	28.52	13.3%	[56]
Single Atom Electrocatalysts					
Ru-SAs/C_3N_4	0.5 M NaOH	-0.05	23	8.3%	[57]
Au-SAs/C_3N_4	0.005M H_2SO_4	-0.2	1305 ug h^{-1} mg_{Au}^{-1}	11.1%	[58]
Fe-SA/NC	0.1 M KOH	0	7.48	56.55%	[59]
Fe_1-NC	0.1 M HCl	-0.3	4.97	4.51%	[60]
FeTPPCl	0.1 M Na_2SO_4	-0.3	18.28	16.76%	[61]
Fe-SA/LCC/GC	0.1 M KOH	-0.1	32.1	29.3%	[62]
Cu-SA/NC	0.1 M HCl	-0.3	49.3	11.7%	[63]
MoSA-Mo_2C/ NCNTs	0.1 M K_2SO_4+ 0.005M H_2SO_4	-0.25	16.1	7.15%	[64]
Co-SA/NC-500	0.1 M KOH	-0.4	5.1	10.1%	[65]
Co-Mo-SA/NC	**0.1 M Na_2SO_4**	**-0.1**	**37.73**	**23.18%**	**This work**

E/V vs RHE	-0.6	-0.5	-0.4	-0.3	-0.2	-0.1	0.0
1	8.06	10.08	14.06	18.35	21.62	39.46	7.27
2	6.77	8.89	13.04	17.98	23.83	36.52	8.38
3	7.29	9.34	12.21	18.42	23.20	37.17	8.53
4	7.94	8.37	12.69	16.68	22.01	36.45	8.07
5	7.32	6.99	13.35	16.96	21.58	38.39	7.09
6	8.22	9.71	13.73	17.75	23.37	38.41	7.82
Average	7.60	9.23	13.18	17.69	22.60	37.73	7.86
Std. Dev.	0.56	0.61	0.68	0.72	0.98	1.20	0.58

Table S3. Partial NH_3 yield rate (ug h^{-1} mg^{-1}) for Co-Mo-SA/NC.

Table S4. Partial faradaic efficiency (%) for Co-Mo-SA/NC.

E/V vs RHE	-0.6	-0.5	-0.4	-0.3	-0.2	-0.1	0.0
1	0.13	0.89	2.57	4.91	11.10	24.39	0.12
2	0.15	0.86	2.43	5.17	12.38	22.68	0.07
3	0.17	0.75	2.04	4.06	10.82	22.57	0.17
4	0.19	0.84	2.08	4.32	11.59	23.85	0.15
5	0.09	0.66	2.55	5.15	12.53	22.16	0.05
6	0.08	0.70	2.19	4.23	11.96	23.43	0.07
Average	0.14	0.79	2.31	4.64	11.73	23.18	0.11
Std. Dev.	0.04	0.10	0.24	0.49	0.69	0.85	0.05

Table S5. The calculated zero-point energies (ZPE) and entropy correction (-TS) of different adsorption species for Co-Mo-SA/NC, where the * represents the catalyst, *N≡*N and *N≡N refer to the side-on and end-on adsorption configurations, respectively.

Adsorption structure	E_{ZPE} (eV)	$-TS$ (eV)
N_2	0.15	-0.58
*N≡*N	0.19	-0.12
*N=*NH	0.49	-0.13
*NH =*NH	0.79	-0.16
NH−NH_2	1.11	-0.25
NH_2−NH_2	1.35	-0.20
*N	0.09	-0.06
*NH	0.35	-0.09
*NH_2	0.65	-0.13
*NH_3	1.00	-0.15
*N≡N	0.21	-0.15
*N=NH	0.47	-0.18
*N−NH_2	0.81	-0.21
NH_3	0.58	-0.56

Table S6. Comparisons of calculated NRR limiting potential for Co-Mo-SA/NC with recently reported electrocatalysts.

Catalyst	Calculated NRR limiting potentials	Reference
Fe-B_2N_4	-0.65 V	66
Re@MoS_2	-0.43 V	67
Cr-C_2N_2	-0.40 V	68
Ti/g-CN	-0.39 V	69
W-N_2O_2	-0.30 V	70
W@C_9N_4	-0.24 V	71
Fe-SAC	-0.30 V	72
F-Fe@F-G	-0.36 V	73
Fe-Ru/NC	-0.39 V	74
Co-Mo-SA/NC	-0.33 V	This Work

References

1. W. Qiu, X. Y. Xie, J. Qiu, W. H. Fang, R. Liang, X. Ren, X. Ji, G. Cui, A. M. Asiri, G. Cui, B. Tang and X. Sun, *Nat. Commun.*, 2018, **9**, 3485.
2. X. Zhu, T. Wu, L. Ji, C. Li, T. Wang, S. Wen, S. Gao, X. Shi, Y. Luo, Q. Peng and X. Sun, *J. Mater. Chem. A*, 2019, **7**, 16117-16121.
3. L. Zhang, L. X. Ding, G. F. Chen, X. Yang and H. Wang, *Angew. Chem. Int. Ed. Engl.*, 2019, **58**, 2612-2616.
4. X. Zhang, T. Wu, H. Wang, R. Zhao, H. Chen, T. Wang, P. Wei, Y. Luo, Y. Zhang and X. Sun, *ACS Catal.*, 2019, **9**, 4609-4615.
5. X. Yu, P. Han, Z. Wei, L. Huang, Z. Gu, S. Peng, J. Ma and G. Zheng, *Joule*, 2018, **2**, 1610-1622.
6. Y. Liu, Y. Su, X. Quan, X. Fan, S. Chen, H. Yu, H. Zhao, Y. Zhang and J. Zhao, *ACS Catal.*, 2018, **8**, 1186-1191.
7. D. Yuan, Z. Wei, P. Han, C. Yang, L. Huang, Z. Gu, Y. Ding, J. Ma and G. Zheng, *J. Mater. Chem. A*, 2019, **7**, 16979-16983.
8. C. Lv, Y. Qian, C. Yan, Y. Ding, Y. Liu, G. Chen and G. Yu, *Angew. Chem. Int. Ed. Engl.*, 2018, **57**, 10246-10250.
9. Y. Wen, H. Zhu, J. Hao, S. Lu, W. Zong, F. Lai, P. Ma, W. Dong, T. Liu and M. Du, *Appl. Catal. B*, 2021, **292**.
10. B. Chang, L. Li, D. Shi, H. Jiang, Z. Ai, S. Wang, Y. Shao, J. Shen, Y. Wu, Y. Li and X. Hao, *Appl. Catal. B*, 2021, **283**.
11. H. Zhao, D. Zhang, H. Li, W. Qi, X. Wu, Y. Han, W. Cai, Z. Wang, J. Lai and L. Wang, *Adv. Energy Mater.*, 2020, **10**.
12. W. Xu, G. Fan, J. Chen, J. Li, L. Zhang, S. Zhu, X. Su, F. Cheng and J. Chen, *Angew. Chem. Int. Ed. Engl.*, 2020, **59**, 3511-3516.
13. Z. H. Xue, S. N. Zhang, Y. X. Lin, H. Su, G. Y. Zhai, J. T. Han, Q. Y. Yu, X. H. Li, M. Antonietti and J. S. Chen, *J. Am. Chem. Soc.*, 2019, **141**, 14976-14980.
14. H. Wang, H. Yu, Z. Wang, Y. Li, Y. Xu, X. Li, H. Xue and L. Wang, *Small Methods*, 2019, **15**, e1804769.
15. M. M. Shi, D. Bao, B. R. Wulan, Y. H. Li, Y. F. Zhang, J. M. Yan and Q. Jiang, *Adv. Mater.*, 2017, **29**.
16. J. Zheng, Y. Lyu, M. Qiao, J. P. Veder, R. D. Marco, J. Bradley, R. Wang, Y. Li, A. Huang, S. P. Jiang and S. Wang, *Angew. Chem. Int. Ed. Engl.*, 2019, **58**, 18604-18609.
17. M. Nazemi and M. A. El-Sayed, *J Phys Chem Lett*, 2018, **9**, 5160-5166.
18. J. Wang, L. Yu, L. Hu, G. Chen, H. Xin and X. Feng, *Nat. Commun.*, 2018, **9**, 1795.
19. M. Ma, X. Han, H. Li, X. Zhang, Z. Zheng, L. Zhou, J. Zheng, Z. Xie, Q. Kuang and L. Zheng, *Appl. Catal. B*, 2020, **265**.
20. P. Wang, W. Nong, Y. Li, H. Cui and C. Wang, *Appl. Catal. B*, 2021, **288**.
21. M.-M. Shi, D. Bao, S.-J. Li, B.-R. Wulan, J.-M. Yan and Q. Jiang, *Adv. Energy Mater.*, 2018, **8**.
22. X. Wang, M. Luo, J. Lan, M. Peng and Y. Tan, *Adv. Mater.*, 2021, **33**.
23. F. Pang, Z. Wang, K. Zhang, J. He, W. Zhang, C. Guo and Y. Ding, *Nano Energy*, 2019, **58**, 834-841.
24. D. Bao, Q. Zhang, F. L. Meng, H. X. Zhong, M. M. Shi, Y. Zhang, J. M. Yan, Q. Jiang and X. B. Zhang, *Adv. Mater.*, 2017, **29**.
25. S. J. Li, D. Bao, M. M. Shi, B. R. Wulan, J. M. Yan and Q. Jiang, *Adv. Mater.*, 2017, **29**.
26. D. Zhang, H. Zhao, X. Wu, Y. Deng, Z. Wang, Y. Han, H. Li, Y. Shi, X. Chen, S. Li, J. Lai, B. Huang and L. Wang, *Adv. Funct. Mater.*, 2020, **31**.
27. H. Tao, C. Choi, L.-X. Ding, Z. Jiang, Z. Han, M. Jia, Q. Fan, Y. Gao, H. Wang, A. W. Robertson, S. Hong, Y. Jung, S. Liu and Z. Sun, *Chem*, 2019, **5**, 204-214.

28. B. H. R. Suryanto, D. Wang, L. M. Azofra, M. Harb, L. Cavallo, R. Jalili, D. R. G. Mitchell, M. Chatti and D. R. MacFarlane, *ACS Energy Lett.*, 2018, **4**, 430-435.
29. H. Huang, L. Xia, X. Shi, A. M. Asiri and X. Sun, *Chem. Commun.*, 2018, **54**, 11427-11430.
30. H.-M. Liu, S.-H. Han, Y. Zhao, Y.-Y. Zhu, X.-L. Tian, J.-H. Zeng, J.-X. Jiang, B. Y. Xia and Y. Chen, *J. Mater. Chem. A*, 2018, **6**, 3211-3217.
31. Y. Gu, B. Xi, W. Tian, H. Zhang, Q. Fu and S. Xiong, *Adv. Mater.*, 2021, DOI: 10.1002/adma.202100429, e2100429.
32. Y. Guo, Z. Yao, B. J. J. Timmer, X. Sheng, L. Fan, Y. Li, F. Zhang and L. Sun, *Nano Energy*, 2019, **62**, 282-288.
33. C. Lv, C. Yan, G. Chen, Y. Ding, J. Sun, Y. Zhou and G. Yu, *Angew. Chem. Int. Ed. Engl.*, 2018, **57**, 6073-6076.
34. J. X. Yao, D. Bao, Q. Zhang, M. M. Shi, Y. Wang, R. Gao, J. M. Yan and Q. Jiang, *Small Methods*, 2018, **3**.
35. Y. T. Liu, L. Tang, J. Dai, J. Yu and B. Ding, *Angew. Chem. Int. Ed. Engl.*, 2020, **59**, 13623-13627.
36. B. Qin, Y. Li, Q. Zhang, G. Yang, H. Liang and F. Peng, *Nano Energy*, 2020, **68**.
37. Y. X. Luo, W. B. Qiu, R. P. Liang, X. H. Xia and J. D. Qiu, *ACS Appl. Mater. Interfaces*, 2020, **12**, 17452-17458.
38. S. Chen, S. Perathoner, C. Ampelli, C. Mebrahtu, D. Su and G. Centi, *Angew. Chem. Int. Ed. Engl.*, 2017, **56**, 2699-2703.
39. C. He, Z.-Y. Wu, L. Zhao, M. Ming, Y. Zhang, Y. Yi and J.-S. Hu, *ACS Catal.*, 2019, **9**, 7311-7317.
40. P. Song, H. Wang, L. Kang, B. Ran, H. Song and R. Wang, *Chem. Commun.*, 2019, **55**, 687-690.
41. H. Jin, L. Li, X. Liu, C. Tang, W. Xu, S. Chen, L. Song, Y. Zheng and S. Z. Qiao, *Adv. Mater.*, 2019, **31**, e1902709.
42. H. Cheng, L. X. Ding, G. F. Chen, L. Zhang, J. Xue and H. Wang, *Adv. Mater.*, 2018, **30**, e1803694.
43. X. Li, T. Li, Y. Ma, Q. Wei, W. Qiu, H. Guo, X. Shi, P. Zhang, A. M. Asiri, L. Chen, B. Tang and X. Sun, *Adv. Energy Mater.*, 2018, **8**.
44. Z. Zhao, S. Luo, P. Ma, Y. Luo, W. Wu, Y. Long and J. Ma, *ACS Sustain. Chem. Eng.*, 2020, **8**, 8814-8822.
45. Y. Liu, M. Han, Q. Xiong, S. Zhang, C. Zhao, W. Gong, G. Wang, H. Zhang and H. Zhao, *Adv. Energy Mater.*, 2019, **9**.
46. D. Yang, T. Chen and Z. Wang, *J. Mater. Chem. A*, 2017, **5**, 18967-18971.
47. Y. Gao, Z. Han, S. Hong, T. Wu, X. Li, J. Qiu and Z. Sun, *ACS Appl. Energy Mater.*, 2019, **2**, 6071-6077.
48. Q. Qin, Y. Zhao, M. Schmallegger, T. Heil, J. Schmidt, R. Walczak, G. Gescheidt-Demner, H. Jiao and M. Oschatz, *Angew. Chem. Int. Ed. Engl.*, 2019, **58**, 13101-13106.
49. Y. Fang, Z. Liu, J. Han, Z. Jin, Y. Han, F. Wang, Y. Niu, Y. Wu and Y. Xu, *Adv. Energy Mater.*, 2019, **9**.
50. M. Yuan, Q. Li, J. Zhang, J. Wu, T. Zhao, Z. Liu, L. Zhou, H. He, B. Li and G. Zhang, *Adv. Funct. Mater.*, 2020, **30**.
51. Y. X. Lin, S. N. Zhang, Z. H. Xue, J. J. Zhang, H. Su, T. J. Zhao, G. Y. Zhai, X. H. Li, M. Antonietti and J. S. Chen, *Nat. Commun.*, 2019, **10**, 4380.
52. Z. Jiang, W. Sun, H. Shang, W. Chen, T. Sun, H. Li, J. Dong, J. Zhou, Z. Li, Y. Wang, R. Cao, R. Sarangi, Z. Yang, D. Wang, J. Zhang and Y. Li, *Energy Environ. Sci.*, 2019, **12**, 3508-3514.
53. M. Qin, X. Li, G. Gan, L. Wang, S. Fan, Z. Yin and G. Chen, *ACS Sustain. Chem. Eng.*, 2020, **8**, 13430-13439.

54. X. Liu, H. Jang, P. Li, J. Wang, Q. Qin, M. G. Kim, G. Li and J. Cho, *Angew. Chem. Int. Ed. Engl.*, 2019, **58**, 13329-13334.
55. M. Zhang, Y. Wang, Y. Zhang, J. Song, Y. Si, J. Yan, C. Ma, Y. T. Liu, J. Yu and B. Ding, *Angew. Chem. Int. Ed. Engl.*, 2020, **59**, 23252-23260.
56. H. Xian, H. Guo, J. Xia, Q. Chen, Y. Luo, R. Song, T. Li and E. Traversa, *ACS Appl. Mater. Interfaces*, 2021, **13**, 7142-7151.
57. Z. Geng, Y. Liu, X. Kong, P. Li, K. Li, Z. Liu, J. Du, M. Shu, R. Si and J. Zeng, *Adv. Mater.*, 2018, DOI: 10.1002/adma.201803498, e1803498.
58. X. Wang, W. Wang, M. Qiao, G. Wu, W. Chen, T. Yuan, Q. Xu, M. Chen, Y. Zhang, X. Wang, J. Wang, J. Ge, X. Hong, Y. Li, Y. Wu and Y. Li, *Sci. Bull.*, 2018, **63**, 1246-1253.
59. M. Wang, S. Liu, T. Qian, J. Liu, J. Zhou, H. Ji, J. Xiong, J. Zhong and C. Yan, *Nat. Commun.*, 2019, **10**, 341.
60. R. Zhang, L. Jiao, W. Yang, G. Wan and H.-L. Jiang, *J. Mater. Chem. A*, 2019, **7**, 26371-26377.
61. X. Yang, S. Sun, L. Meng, K. Li, S. Mukherjee, X. Chen, J. Lv, S. Liang, H.-Y. Zang, L.-K. Yan and G. Wu, *Appl. Catal. B*, 2021, **285**.
62. B. Yu, H. Li, J. White, S. Donne, J. Yi, S. Xi, Y. Fu, G. Henkelman, H. Yu, Z. Chen and T. Ma, *Adv. Funct. Mater.*, 2019, **30**.
63. W. Zang, T. Yang, H. Zou, S. Xi, H. Zhang, X. Liu, Z. Kou, Y. Du, Y. P. Feng, L. Shen, L. Duan, J. Wang and S. J. Pennycook, *ACS Catal.*, 2019, **9**, 10166-10173.
64. Y. Ma, T. Yang, H. Zou, W. Zang, Z. Kou, L. Mao, Y. Feng, L. Shen, S. J. Pennycook, L. Duan, X. Li and J. Wang, *Adv. Mater.*, 2020, **32**, e2002177.
65. Y. Liu, Q. Xu, X. Fan, X. Quan, Y. Su, S. Chen, H. Yu and Z. Cai, *J. Mater. Chem. A*, 2019, **7**, 26358-26363.
66. D. Jiao, Y. Liu, Q. Cai and J. Zhao, *J. Mater. Chem. A*, 2021, **9**, 1240-1251.
67. W. Song, K. Xie, J. Wang, Y. Guo, C. He and L. Fu, *Phys. Chem. Chem. Phys.*, 2021, **23**, 10418-10428.
68. W. Nong, S. Qin, F. Huang, H. Liang, Z. Yang, C. Qi, Y. Li and C. Wang, *Carbon*, 2021, **182**, 297-306.
69. H. Niu, Z. Zhang, X. Wang, X. Wan, C. Shao and Y. Guo, *Adv. Funct. Mater.*, 2020, **31**.
70. Y. Gu, B. Xi, W. Tian, H. Zhang, Q. Fu and S. Xiong, *Adv Mater*, 2021, **33**, e2100429.
71. Z. Xue, X. Zhang, J. Qin and R. Liu, *Nano Energy*, 2021, **80**.
72. Z. Y. Wu, M. Karamad, X. Yong, Q. Huang, D. A. Cullen, P. Zhu, C. Xia, Q. Xiao, M. Shakouri, F. Y. Chen, J. Y. T. Kim, Y. Xia, K. Heck, Y. Hu, M. S. Wong, Q. Li, I. Gates, S. Siahrostami and H. Wang, *Nat. Commun.*, 2021, **12**, 2870.
73. X. Wang, Y. Zhao, L. Wang, W. Peng, J. Feng, D. Li, B. J. Su, J. Y. Juang, Y. Ma, Y. Chen, F. Hou, S. Zhou, H. K. Liu, S. X. Dou, J. Liu and J. Liang, *Adv. Funct. Mater.*, 2022, DOI: 10.1002/adfm.202111733.
74. B. Tha, C. Arps and B. Ada, *J. Cataly.*, 2020, **388**, 77-83.